NUMERICAL INVESTIGATION OF HYDROGEN LEAKAGE FROM A HIGH PRESSURE TANK AND ITS EXPLOSION

Taira Y.[1], Saburi T.[2], Kubota S.[3], Sugiyama Y.[4] and Matsuo A.[5]
[1] Graduate School of Science and Technology, Keio University, 3-14-1 Hiyoshi, Kohoku, Yokohama, Kanagawa 223-8522, Japan, 19911029@keio.jp
[2] Research Institute of Science for Safety and Sustainability, National Institute of Advanced Industrial Science and Technology, 16-1 Onogawa, Tsukuba, Ibaraki 305-8569, Japan, t.saburi@aist.go.jp
[3] Research Institute of Science for Safety and Sustainability, National Institute of Advanced Industrial Science and Technology, 16-1 Onogawa, Tsukuba, Ibaraki 305-8569, Japan, kubota.46@aist.go.jp
[4] Research Institute of Science for Safety and Sustainability, National Institute of Advanced Industrial Science and Technology, 16-1 Onogawa, Tsukuba, Ibaraki 305-8569, Japan, yuta.sugiyama@aist.go.jp
[5] Department of Mechanical Engineering, Keio University, 3-14-1 Hiyoshi, Kohoku, Yokohama, Kanagawa 223-8522, Japan, matsuo@mech.keio.ac.jp

ABSTRACT

We numerically investigated the initial behavior of leakage and diffusion from high-pressure hydrogen storage tank assumed in hydrogen station. First, calculations are carried out to validate the present numerical approach and compare with the theoretical distribution of hydrogen mass fraction to the direction**,** which is vertical to the jet direction**,** in the case of hydrogen leaking out from the circular injection port, whose diameter is 0.25 mm. Then, performing calculations about hydrogen leakage and diffusion behavior on different tank pressures, the effects are examined to reduce damage by gas explosion assumed in the hydrogen station. There is no significant difference in the diffusion distance to the jet direction from a start to 0.2 ms. After 0.2 ms, it is seen the difference in the diffusion distance to the jet direction in different pressure. As tank pressures become large, the hydrogen diffusion not only to the jet direction but also to the direction, which is vertical to the jet direction, is remarkably seen. Then, according to histories of the percentage of the flammable mass to total one in the space, it drastically increases up to 30% between 0 and 0.05 ms. After 0.05 ms, it uniformly increases, so it is shown that the explosion risk becomes high over time. The place where mass within flammability range distributes at a certain time is shown. Hydrogen widely diffuses to jet direction and distributes in each case and time. Therefore, it is found that when it is assumed that ignition occurs by some sources in place where high-pressure hydrogen is leaked and diffused, the magnitude of the explosion damage can be predicted when and where ignition occurs.

1.0 INTRODUCTION

In the 21st century, the increases in population and industrialization in developing countries raise the energy consumption and the demands for renewable energy instead of fossil fuels. The new technology to use hydrogen as the energy source is developing. Hydrogen is expected not only to be an alternative to fossil fuels but also to be a resolution of the environmental issues such as global warming and atmospheric pollution, because it does not emit harmful gases to the environment such as CO, CO_2, NO_X, and SO_X when it burns. In particular, when energy from hydrogen is introduced to the transport sector like fuel cell vehicles (following FCV), the installation of hydrogen station in urban areas is being promoted in Japan. The hydrogen station is a facility to provide hydrogen for FCV, and hydrogen is produced, stored, and utilized there. Hydrogen stored there is compressed at high pressure, such as 70 MPa. When gas generally becomes high-pressure, the amount of storage gas becomes large. On the other hand, high-pressure hydrogen may leak from the tank because of tank rapture. Moreover, the flammability range of hydrogen-air mixtures (from 4 to 75 vol.%) is much larger than hydrocarbon fuel-air mixtures such as methane and propane and its minimum ignition energy is order of 10^{-2} mJ, which is much smaller than hydrocarbon fuel-air mixtures. Also, the diffusion coefficient of hydrogen into air is larger than hydrocarbon fuel-air mixtures. Therefore, hydrogen leakage from high-pressure tank in hydrogen stations would cause serious hazard. Many theoretical, experimental, and numerical studies have been conducted and some experiments have studied diffusion behavior at different tank

pressure and leakage hole diameter. However, experimental approach requires costs and it is especially difficult to observe the hydrogen concentration diffusing in large space such as the atmosphere. Numerical simulation, on the other hand, can require lower costs and provide a detailed flow field. Chernyavsky *et al.* conducted numerical investigation of subsonic hydrogen jet release [1]. Also, Takeno *et al.* carried out experiments at various conditions in tank pressure and leak diameter and showed empirical formula between hydrogen diffusion distance and concentration on axis in a steady state by Mitsubishi Heavy Industries [2],[3]. There is a lack of experiments or simulations for hydrogen diffusion distance in real scale assuming a hydrogen station. Therefore, this study aims to clarify the diffusion behavior in different tank pressure and evaluate the diffusion and explosion damage assumed in the hydrogen station.

2.0 NUMERICAL DETAILS

2.1 Computational target and calculation conditions

The computational target is hydrogen diffusion behavior in the atmosphere from a leakage hole of high-pressure hydrogen storage tank assumed in the hydrogen station. An example of grids used in this numerical simulation is shown in Fig. 1, and it also shows boundary conditions. Grids are shown in every 3 points. The *yz* plane with a leakage hole center of high-pressure hydrogen storage tank is adiabatic no-slip wall condition, and symmetry condition is applied to the center of the cross section for the reduction of the calculation load. The symmetric condition does not affect histories of hydrogen diffusion distance, when it is compared with histories of the distance without the symmetry condition as shown in the section 3.1. The other boundaries are 0^{th} extrapolation as outflow condition. The minimum grid size is 0.02 mm and total grid points are about 2,100,000 (*x* direction 182 x *y* direction 147 x *z* direction 78). Since physical quantities rapidly change around the jet inlet point, the grid interval places finely around it. After constant distances, grid size is stretched in common ratio 1.05. Grid stretch ratio is changed into 1.5 after taking a certain distance, and the wide computational domain is taken. The atmospheric condition is shown in Table 1, and hydrogen jet conditions in the section 3.1 and 3.2 are shown in Table 2, 3 respectively. Mach number in the injection port is 1.0, because the injection port is considered to choke from the ratio of hydrogen jet pressure to atmospheric pressure. High-pressure hydrogen is injected from the circular injection port on the choked condition that injection pressure, temperature and injection mass flow rate are constant. It is possible to consider that the decrease of tank pressure and mass flow rate is negligible in the range of the calculated time in this study. Therefore, it is regarded as constant pressure and mass flow rate. Fig. 2 shows the model of hydrogen leakage and diffusion behavior. Since choke occurs at the circular injection port, it is shown the relations between p_0 and p_e in Eq. (1) and the relations between T_0 and T_e in Eq. (2).

$$\frac{p_e}{p_0} = \left(\frac{2}{\gamma + 1} \right)^{\frac{\gamma}{\gamma - 1}} , \tag{1}$$

$$\frac{T_e}{T_0} = \frac{2}{\gamma + 1} , \tag{2}$$

where p_0 – tank pressure, Pa; p_e – pressure in injection port outlet, Pa; T_0 – tank temperature, K; T_e – temperature in injection port outlet, K; γ – the specific heat ratio.

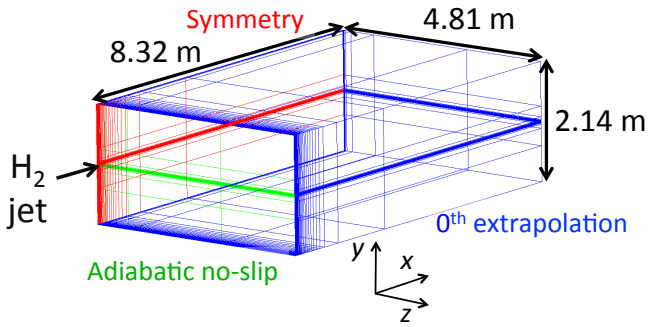

Figure 1. Example of computational grids shown in every 3 points and boundary conditions

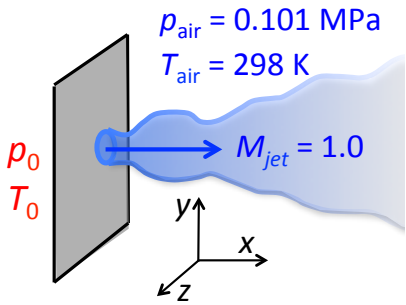

Figure 2. Hydrogen leakage and diffusion model from high-pressure tank

Table 1. Atmospheric condition

Pressure [MPa]	0.1013
Temperature [K]	298
Gas species	Air (O_2 : N_2 = 1: 3.76)

Table 2. Hydrogen jet condition (Section 3.1)

Mach number [-]	1.0
Tank pressure [MPa]	3.463
Tank temperature [K]	354
Mass flow rate [kg/s]	9.64×10^{-5}
Jet speed [m/s]	1323
Gas species	H_2

Table 3. Hydrogen jet condition (Section 3.2)

Mach number [-]	1.0		
Tank pressure [MPa]	1.825	3.650	7.300
Tank temperature [K]	294		
Mass flow rate [kg/s]	5.58×10^{-5}	1.12×10^{-4}	2.23×10^{-4}
Jet speed [m/s]	1207		
Gas species	H_2		

2.2 Governing equations

The governing equations are 3D compressible Favre filtered Navier-Stokes equations, and equations of chemical species conservation. Subscript k in equations of chemical species conservation is the number of considered chemical species, it deals with 3 chemical species, H_2, N_2, and O_2 in this study. Favre filtered equations of mass, momentum, energy and chemical species conservation are shown as follows.

$$\frac{\partial \bar{\rho}}{\partial t} + \frac{\partial \bar{\rho}\tilde{u}_i}{\partial x_i} = 0 \ , \tag{3}$$

$$\frac{\partial\left(\bar{\rho}\tilde{u}_i\right)}{\partial t} + \frac{\partial\left(\bar{\rho}\tilde{u}_i\tilde{u}_j + \delta_{ij}\bar{p}\right)}{\partial x_i} = \frac{\partial}{\partial x_i}\left[2\left(\mu + \mu_{SGS}\right)\left(\tilde{S}_{ij} - \delta_{ij}\frac{1}{3}\tilde{S}_{kk}\right)\right] , \tag{4}$$

$$\frac{\partial \bar{e}}{\partial t} + \frac{\partial\left(\bar{e} + \bar{p}\right)\tilde{u}_i}{\partial x_i} = \frac{\partial}{\partial x_i}\left[\left(\frac{\mu}{\mathrm{Pr}} + \frac{\mu_{SGS}}{\mathrm{Pr}_{SGS}}\right)\frac{\partial \tilde{h}}{\partial x_i} + 2\mu\tilde{u}_i\left(\tilde{S}_{ij} - \delta_{ij}\frac{1}{3}\tilde{S}_{kk}\right)\right] , \tag{5}$$

$$\frac{\partial \bar{\rho}_k}{\partial t} + \frac{\partial \bar{\rho}_k\tilde{u}_i}{\partial x_i} = \frac{\partial}{\partial x_i}\left(\bar{\rho}_k D_k \frac{\partial \bar{Y}_k}{\partial x_i}\right) , \tag{6}$$

where t – time, s; x_i – spatial coordinate, m; ρ – density, kg/m^3; u_i – velocity, m/s; p – pressure, Pa; μ – viscosity, kg/m/s; μ_{SGS} – SGS viscosity, kg/m/s; S_{ij} – strain tensor, 1/s; e – total energy per unit volume, J/m^3, Pr – Prandtl number, Pr_{SGS} – SGS Prandtl number, h – enthalpy, J/kg; ρ_k – density of chemical species k, kg/m^3; D_k – diffusion coefficient of chemical species k in mixed gas, m^2/s; Y_k – mass fraction of chemical species k.

The overbar denotes spatial filterling, and the tilde denotes mass-weighted filtering. The turbulence model is LES [4],[5]. In this study, mixed time scale model is used for SGS turbulent stress model. Discretization method for the convective term is third-order SHUS [6], which is one of the AUSM family schemes [7]. Time integration method is 3 step Runge-Kutta method [8].

3.0 RESULTS AND DISCUSSION

3.1 Study of hydrogen jet condition

In this study, high-pressure hydrogen is injected at the sonic speed from the circular injection port, whose diameter is 0.25 mm. Here, the grid refinement study is carried out to clarify the grid resolution to simulate the diffusion process of hydrogen released from high-pressure storage tank. Five kinds of computational resolution are prepared. The circular port is represented by the square grid as shown in Fig. 3, and 1, 5, 9, 13 and 17 grids are used for the diameter of hydrogen injection port ($D/dx =$ 1, 5, 9, 13, 17; D: diameter, dx: grid width). The hydrogen is injected in grids assuming the circle of 0.25 mm diameter, and therefore coefficient of discharge is applied to fit the ideal mass flow. At first, the jet behavior on the jet direction is examined. The location of hydrogen mole fraction of 0.04 is tracked on the axis, and the histories of five cases are plotted in Fig. 4. The histories in the case of $D/dx =$ 1, 5 are different from the other cases, and seems to be non-physical. However, other cases do not change very much. Next, the jet distribution on y-z plane is examined in the cases of $D/dx =$ 9, 13 and 17. The distributions of hydrogen mass fraction are plotted in y-direction on x = 10 mm at 0.11 ms in Fig. 5. The distance of y is normalized by the jet half-width, L_y, and the hydrogen mass fraction is normalized by the mass fraction on jet axis at x = 10 mm, Y_c. At 0.11 ms, the flow field has been already developed at x = 10 mm, and therefore the distribution can be compared with the theoretical profile, which is Gaussian distribution, as seen in Fig. 5. The comparison indicates that the profiles of $D/dx =$ 9 are totally different from the theoretical one, but those of $D/dx =$ 13 and 17 show

favorable. This grid refinement study suggests that grid points inside the diameter are required at least 13 points to reproduce the diffusion process of high-pressure hydrogen from the circular injection port at the sonic speed. Therefore, $D/dx = 13$ conditions is applied to all calculations after this.

Furthermore, the mirror boundary condition is applied to the x-y plane including the x-axis at the center of jet injection port in order to reduce the computational load. Two calculations are performed to confirm the validity of mirror condition; one was done in the whole computation domain and the other is in the half, and the comparison of histories of the distance on jet axis from the injection port to the location of hydrogen mole fraction of 0.04 in the case of $D/dx = 13$ is carried out, as seen in Fig. 6. The figure says that the lines are almost the same and therefore the use of mirror condition is reasonable to simulate the hydrogen jet diffusion process.

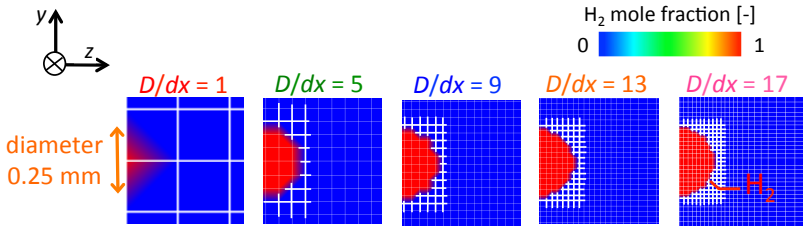

Figure 3. How to simulate the injection port by some grid points in each case

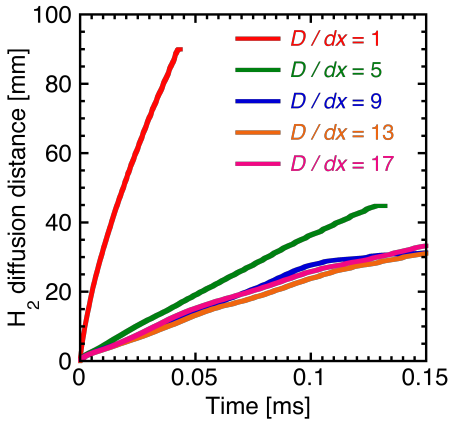

Figure 4. Histories of the distance on jet axis from the injection port to the location of hydrogen mole fraction of 0.04 in 5 cases

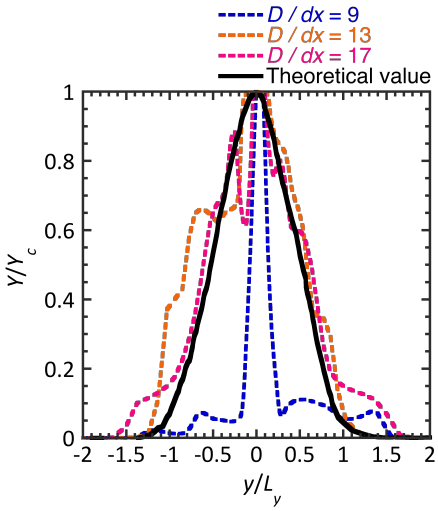

Figure 5. Hydrogen mass fraction distribution in y direction at x = 10 mm, t = 0.11 ms

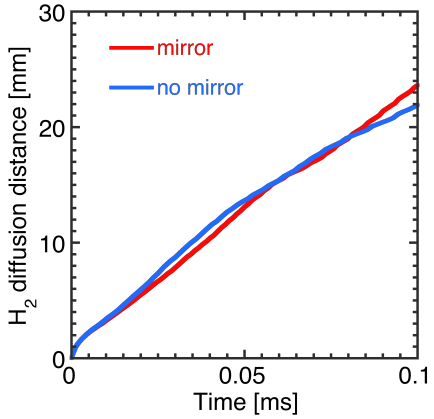

Figure 6. Histories of the distance on jet axis from the injection port
to the location of hydrogen mole fraction of 0.04 between mirror and no mirror condition

3.2 Effects of Tank pressure on Hydrogen leakage

3.2.1. Diffusion distance to jet direction

In this section, the effects of the tank pressure on hydrogen leakage are carried out, and three kinds of hydrogen pressure tank, p_0 = 1.825, 3.650, 7.300 MPa, are examined. Before talking about the computational results, we would like to introduce the previous work based on the experimental data on the hydrogen diffusion by Mitsubishi Heavy Industries [2],[3]. In the experiment, when high-pressure hydrogen at various pressure leaks regularly from small injection port at various diameter, hydrogen concentration in the diffusion region released into the atmosphere is investigated. As shown in Fig. 7(a), organizing the experimental value by using the concentration on jet axis C and steady hydrogen diffusion distance X, the proportional relationship is seen as shown in Eq. (7). Also, θ is the equivalent diameter, which is derived from the injection port diameter D, the density in tank ρ_0, air density ρ_a and the specific heat ratio γ as shown in Eq. (8).

$$C = a\left(\frac{X}{\theta}\right)^{-1}, \tag{7}$$

$$\theta = D\cdot\sqrt{\frac{\rho_0}{\rho_{air}}\cdot\left(\frac{2}{\gamma+1}\right)^{\frac{1}{\gamma-1}}}, \tag{8}$$

where C – the concentration on jet axis at distance X, %; a – proportional constant, X – distance to jet direction, mm; θ – equivalent diameter, mm; D – diameter of the injection port, mm; ρ_0 – density in tank, kg/m^3; ρ_{air} –air density, kg/m^3; γ – the specific heat ratio.

According to the experiment, the proportional constant a is 6400. Using Eq. (7),(8), the relation between the distance to jet direction X and tank pressure p_0 is expressed as shown in Eq.(9).

$$X = \frac{aD}{C}\sqrt{\frac{p_0}{R_0T_0}\cdot\frac{R_{air}T_{air}}{p_{air}}\cdot\left(\frac{2}{\gamma+1}\right)^{\frac{1}{\gamma-1}}}, \tag{9}$$

where p_0 – tank pressure, Pa; R_0 – hydrogen gas constant, J/(kg·K); T_0 – tank temperature, K; p_{air} – atmospheric pressure, Pa; R_{air} – atmospheric gas constant, J/(kg·K); T_{air} – atmospheric temperature, K.

Also, D = 0.25 mm, C = 4%, R_0 = 4124 J/(kg·K), T_0 = 298 K, R_{air} = 287 J/(kg·K), T_{air} = 294 K, p_{air} = 0.1013 MPa and γ = 1.408 are applied in Fig. 7(b). Figure 7(b) shows the relation between the tank

pressure and the hydrogen diffusion distance in a steady state on jet axis. The steady hydrogen diffusion distances on jet axis from the injection port to the location of hydrogen mole fraction of 0.04 are 336.6, 476.2, 673.4 mm on conditions of p_0 = 1.825, 3.650, 7.300 MPa. The steady hydrogen diffusion distance on jet axis obtained from the experiment is in proportion to the square root of tank pressure. On the other hand, it is almost constant regardless of tank pressure in the initial diffusion stage in our numerical simulation as shown in Fig. 8.

Figure 8 shows histories of the distance on jet axis from the injection port to the location of hydrogen mole fraction of 0.04. In these simulations, the hydrogen behavior is the initial diffusion process from a start to 1.1 ms, and then the diffusion distance is increasing during the calculations as seen in Fig.8. Compared to Fig. 7(b), the diffusion distance in our calculation is much shorter than the equilibrium distance in a steady state such as 336.6 mm for p_0 = 1.825 MPa, 476.2 mm for 3.650 MPa and 673.4 mm for 7.300 MPa. First, from a start to 0.2 ms, the behavior of diffusion distance on Fig. 8 does not change very much although the diffusion distance is a function of tank pressure in the explanation of Fig. 7. The physics of the diffusion distance at the initial hydrogen leakage is considered. According to hydrogen jet condition in Table 3, the tank temperature, that is the stagnation temperature, is 294 K and the jet Mach number is 1.0 in all cases. Therefore, the jet speed is constant regardless of the tank pressure, although the mass flow rate depends on the tank pressure. The diffusion velocity to the jet direction, which is derived from the slope of the graph of Fig. 8, is about 250 m/s, and it is about 20 % of the initial jet speed 1207 m/s. The hydrogen sonic jet velocity is much faster than the air sonic jet velocity, and then the jet deceleration process seems to be a dominant factor for the diffusion distance at the beginning. Next, from 0.2 ms to 1.1 ms, it is seen the difference in the diffusion distance to the

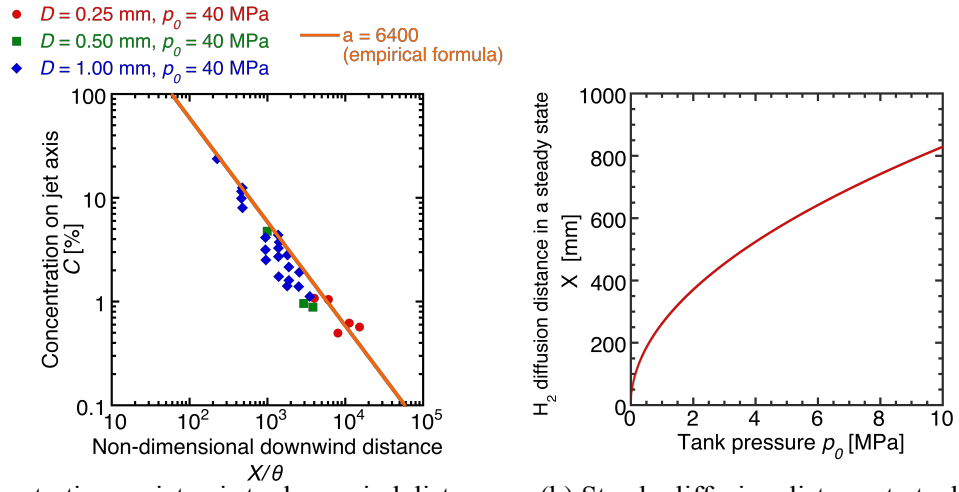

(a) Concentration on jet axis to downwind distance (b) Steady diffusion distance to tank pressure

Figure 7. Relations to the empirical formula by Mitsubishi Heavy Industries [2,3]

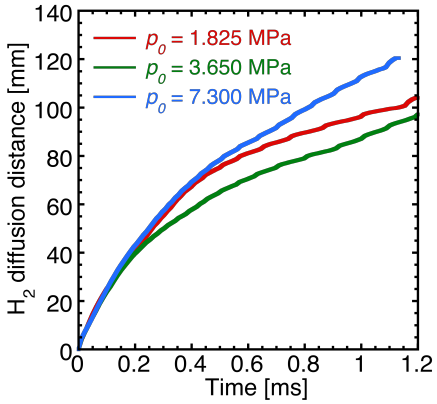

Figure 8. Histories of the distance on jet axis from the injection port to the location of hydrogen mole fraction of 0.04

jet direction in different pressure. So, the velocity of x-component distribution on the jet axis is focused to evaluate the difference behavior between the diffusion distance to the jet direction.

Figure 9 shows the x direction velocity on the jet axis at t = 0.1, 0.6 and 1.1 ms. As mentioned above, the jet speed at the jet port is about 1200 m/s, and it is an under-expansion jet so that the jet expands and accelerates outside the port. In Fig. 9, the jets accelerate near the port and discontinuously decelerate soon in all time. This seems to be the flow path of Mach disk formed in front of the jet port. At t = 0.1 ms, the velocity oscillates after the Mach disk and gradually decelerates regardless of tank pressure. Therefore, it is considered that the diffusion distance to the jet direction does not change very much until 0.2 ms. At t = 0.6, 1.1 ms, the behavior of velocity oscillation shows a different manner after Mach disk depending on the tank pressure. Therefore, it is considered that the diffusion behavior to the jet direction is different in each tank pressure condition after 0.2 ms. Also, the diffusion to the direction which is vertical to the jet direction is implied from the fact that the diffusion distance to the jet direction does not change very much.

Figure 10 shows the time evolving snapshots of hydrogen diffusion behavior on the cross section with the injection center. The diffusion processes in x-y plane in Fig. 10 shows different manners in each tank pressure condition. This comes from the magnitude of mass flow rate. As tank pressure becomes large, hydrogen diffuses to x direction, that is the jet direction, indicating diffusion to y direction which is vertical to the injection direction. Similarly, as tank pressure becomes large, it is seen hydrogen diffusion to z direction.

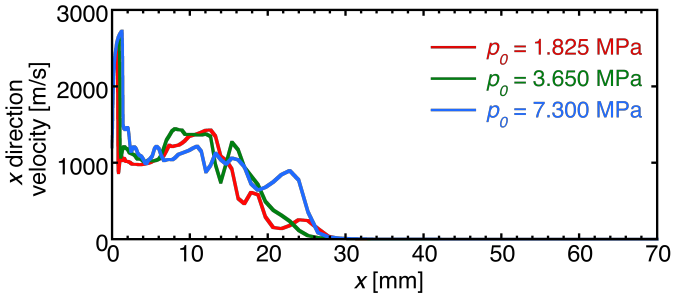

(a) t = 0.1 ms

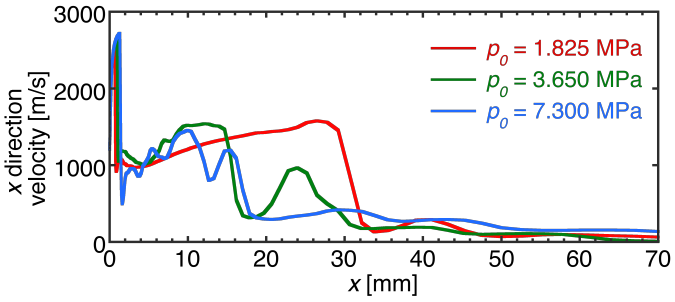

(b) t = 0.6 ms

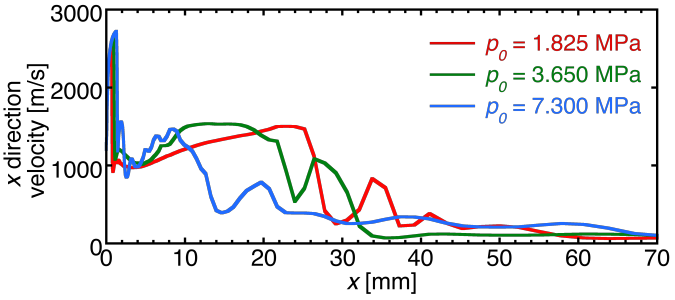

(c) t = 1.1 ms

Figure 9. Jet direction velocity distribution on jet axis in different tank pressure

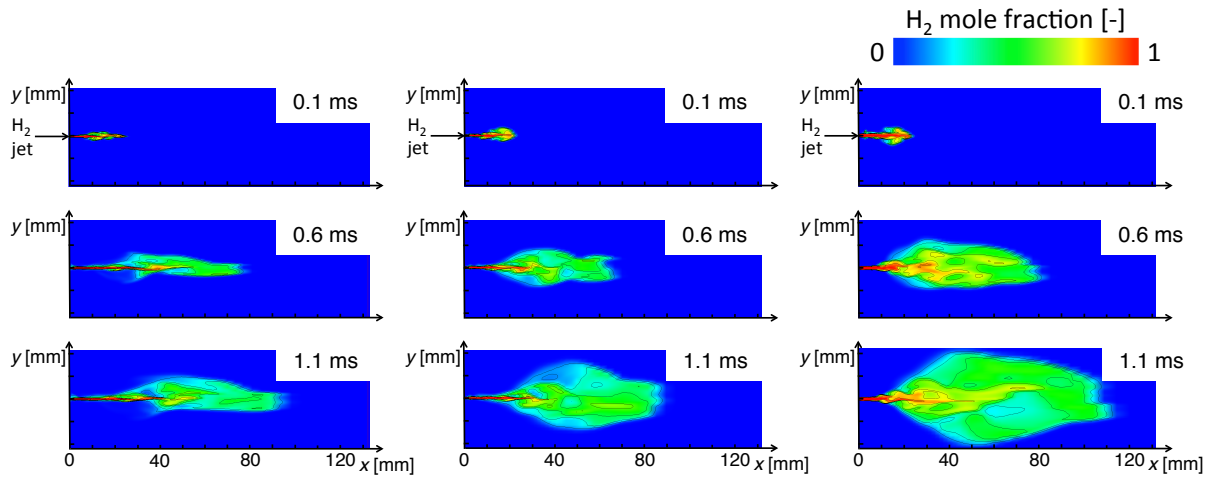

(a) p_0 = 1.825 MPa (b) p_0 = 3.650 MPa (c) p_0 = 7.300 MPa

Figure 10. Time evolving snapshots of hydrogen diffusion behavior on the cross section with the injection center

3.2.2. Estimation of flammability limit distribution

In this section, we focus on the possibility of the explosion caused by hydrogen leakage from the high-pressure storage tank. Characteristics of hydrogen are a wide flammability range of 4-75 vol.%, a small minimum ignition energy and a fast laminar burning velocity, and therefore such characteristics easily cause a serious accident originating from hydrogen leakage. The estimation of the flammable mass spreading in space by hydrogen leakage is one of the important contributions for the computational works to predict damages by explosions.

Figure 11 shows histories of the flammable mass in different tank pressure. The flammable mass is defined using the equivalence ratio ϕ as the stoichiometric mass in case $\phi > 1$ and the stoichiometric mass multiplied ϕ in case $\phi < 1$. The flammable mass spreading in the space uniformly increases in each tank pressure conditions. It is considered that the increase rate of the flammable mass is proportional to the tank pressure because the leakage mass flow rate is also proportional to the tank pressure. Figure 12 shows histories of the percentage of the flammable mass to total one, and the histories do show the same features in three lines. The higher the tank pressure is, the lower the percentage is. This is because the mass under the low flammable limit increases as the diffusion to not only the jet direction but also the direction which is vertical to the jet direction spreads more and more

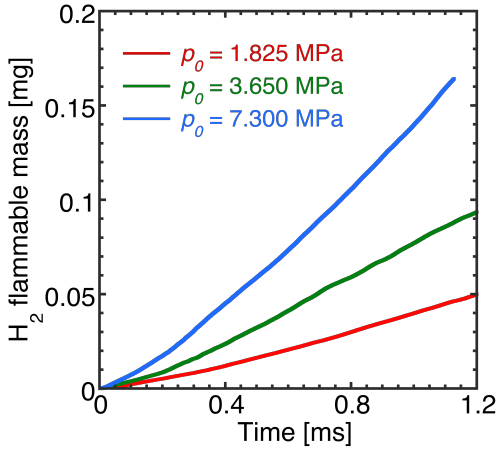

Figure 11. Histories of the flammable mass

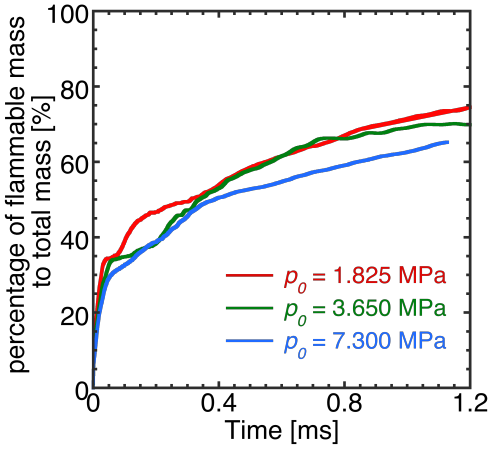

Figure 12. Histories of the percentage of the flammable mass to total one

in higher tank pressure. This figure indicates risk of explosion by the hydrogen leakage from the high-pressure tank, because the mass within the flammable range increases immediately after the start of leakage and get to more than 30% after 0.05 ms. After 0.05 ms, it increases uniformly, so it is shown that the explosion risk becomes high over time. It means that the area, where hydrogen is flowing outward from the jet inlet port, has a possibility to be ignited by the small energy source.

Next, we would like to see the flammable area in y-z space along the jet direction of x-axis. Figure 13 shows the hydrogen mass distribution along x-direction at t = 0.1, 0.6 and 1.1 ms. Moreover, the flammable mass is divided by each x-direction grid width as its width is not uniform. At t = 0.1ms, hydrogen exists between 0 and 25 mm in all cases although the distributions depend on the tank pressure. As mentioned before, there must have Mach disk interactions outside the injection port, and then the oscillation of hydrogen mass is observed. At t = 0.6 and 1.1 ms, the flammable mass range expands forward. At all cases, the flammable mass is not existed very much from an injection port to 5 mm. These figures indicate that where the ignition causes affects the risk of the hydrogen gas explosion by the leakage from the high-pressure tank at initial leakage process.

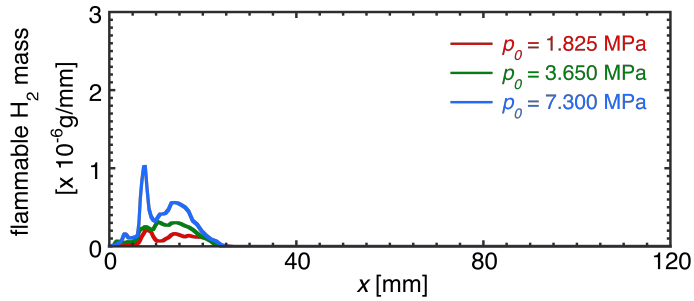

(a) t = 0.1 ms

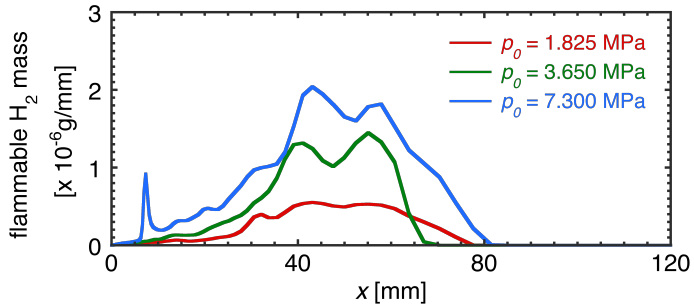

(b) t = 0.6 ms

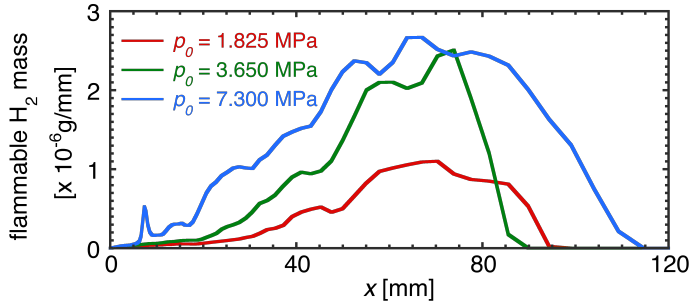

(c) t = 1.1 ms

Figure 13. Distribution of total mass and mass within flammability range in each x cross section

4.0 CONCLUSIONS

A series of numerical investigation on the initial behavior of leakage and diffusion from high-pressure hydrogen storage tank is conducted. The tank pressure is a parameter of the simulations. There is no significant difference in the diffusion distance to jet direction regardless of the difference of the tank pressure from a start to 0.2 ms. After 0.2 ms to 1.1 ms, it is seen the difference in the diffusion distance to the jet direction in different pressure. The x-direction velocity distribution is shown to evaluate these diffusion behaviors. As tank pressures become larger, the hydrogen diffusion not only to the jet direction but also to the direction, which is vertical to the jet direction, is remarkably seen. Then, the flammable mass is investigated to estimate the predicted explosion risk. The flammable mass uniformly increases over time. According to the histories of the percentage of flammable mass to total one, the mass drastically increases up to 30% between 0 and 0.05 ms. After 0.05 ms, it increases uniformly, so it is shown that the explosion risk becomes high over time. The flammable mass distribution along the jet direction is shown to know the risk of where the ignition causes. At t = 0.1ms, hydrogen exists between 0 and 25 mm in all cases although the distributions depend on the tank pressure. At t = 0.6 and 1.1 ms, the flammable mass range expands forward. This work indicates risk of the hydrogen gas explosion by the leakage from the high-pressure tank at the early stage.

REFERENCES

1. Chernyavsky, B., Benard, P., Oshkai, P. and Djilali, N., Numerical Investigation of Subsonic Hydrogen Jet Release, *International Journal of Hydrogen Energy*, **39**, 2014, pp. 6242-6251.
2. Takeno, K., Hashiguchi, K., Okabayashi, K., Chitose, K., Kushiyama, .M. and Noguchi, F., Experimental Study on Open Jet Diffusion Flame and Unconfined Explosion for Leaked High-pressurized Hydrogen, *Journal of Japan Society for Safety Engineering*, **44**, No.6, 2005, pp. 398-406.
3. Okabayashi, K., Takeno, K., Hirashima, H., Chitose, K., Nonaka, T. and Hashiguchi, K., Introduction of Technology for Assessment on Hydrogen Safety, *Mitsubishi Heavy Industries, Ltd. Technical Review,* **44**, No. 1, 2007, pp. 17-19.
4. Erlebacher, G., Hussaini M.Y., Speziale C.G. and Zang T.A., Toward the Large-eddy Simulation of Compressible Turbulent Flows," *Journal of Fluid Mechanics*, **238**, 1992, pp.155-185.
5. Vreman, B., Geurts, B. and Kuerten H., An priori tests of large eddy simulations of the compressible plane mixing layer, *Journal of Engineering Mathematics*, **29**, 1995, pp.299-327.
6. Shima, E. and Kitamura, K., On New Simple Low-Dissipation Scheme of AUSM-Family for All Speeds, *AIAA paper 2009*, **136**, 2009, pp. 1-15.
7. Kitamura K., and Shima E. Improvements of Simple Low-Dissipation AUSM Against Shock Instabilities in Consideration of Interfacial Speed of Sound. Proceedings of 5th European Conference on Computational Fluid Dynamics. Lisbon, Portugal, 14-17 June 2010.
8. Williamson, J.H., Low-Storage Runge-Kutta Scheme, *Journal of Computational Physics*, **35**, 1980, pp. 48-56.